



De Luca, F., Damen, D., Kurton, J., Wray, M., Pokhrel, R., & Werner, M. (2018). TRAFFIC DATA AS PROXY OF BUSINESS DOWNTIME AFTER NATURAL DISASTERS: THE CASE OF KATHMANDU. In *11th National Conference on Earthquake Engineering 2018 (11NCEE): Integrating Science, Engineering, & Policy: Proceedings of a meeting held 25-29 June 2018, Los Angeles, California, USA*. (Vol. 9, pp. 5595-5605). [1287] Earthquake Engineering Research Institute (EERI).

Peer reviewed version

License (if available):
Other

[Link to publication record in Explore Bristol Research](#)
PDF-document

This is the final published version of the article (version of record). It first appeared online via EERI at https://11ncee.org/program?s=TRAFFIC+DATA+AS+PROXY+OF+BUSINESS+DOWNTIME+AFTER+NATURAL+DISASTERS&submit=&option=com_eventprogram&task=Search#ss017s---protective-actions-developing-context-based-guidance-on-what-to-do-during-an-earthquake . Please refer to any applicable terms of use of the publisher.

University of Bristol - Explore Bristol Research

General rights

This document is made available in accordance with publisher policies. Please cite only the published version using the reference above. Full terms of use are available:
<http://www.bristol.ac.uk/pure/about/ebr-terms>



Eleventh U.S. National Conference on Earthquake Engineering
Integrating Science, Engineering & Policy
June 25-29, 2018
Los Angeles, California

TRAFFIC DATA AS PROXY OF BUSINESS DOWNTIME AFTER NATURAL DISASTERS: THE CASE OF KATHMANDU

F. De Luca¹, D. Damen², J. Kurton³, M. Wray⁴, R.M. Pokhrel⁵, M.J.
Werner⁶

ABSTRACT

Traffic data identified from free, satellite imagery, such as historical imagery available on Google Earth, are collected and employed as possible indicator of business downtime after the 2015 Gorkha Earthquake in Nepal. Business downtime is a crucial factor when assessing losses and it is also of great importance to insurance and reinsurance companies, particularly the downtime of private businesses, for which limited data is available. Currently, indicators of business recovery after natural disaster events either focus on damage or they are directly collected through costly procedures and none of the approaches available quantifies longer term recovery. In many cases, such data, when available, are not easy to access. There is a need for both time- and cost-effective methods to quantify business downtime that are not necessarily derived from physical damage and are able to describe both short-term and, potentially, long-term business recovery. The aim of this quantification refers to the recovery phase rather than the immediate emergency response in the aftermath of a natural disaster. Car and lorry numbers of four areas of Kathmandu were counted from historical images available on Google Earth. These four areas correlated to the four areas in which data related to business closures were obtained through interviews during a field investigation made by the authors in Kathmandu in November 2016 (18 months after the event). Food and health business closure data correlate very satisfactory with the calculated drop in car numbers.

¹Lecturer, Dept. of Civil Engineering, University of Bristol, Bristol, BS8 1TR (email: flavia.deluca@bristol.ac.uk)

²Senior Lecturer, Dept. of Computer Science, University of Bristol, Bristol, BS8 1UB

³Undergraduate Student Researcher, Dept. of Civil Engineering, , University of Bristol, Bristol, BS8 1TR

⁴PhD Student, Dept. of Computer Science, University of Bristol, Bristol, BS8 1UB

⁵CEO, Earth Investigation and Solutions Nepal Pvt. Ltd, GPO. Box No. 9261, Kathmandu, Nepal

⁶Senior Lecturer, School Earth Sciences, University of Bristol, Bristol, BS8 1TRJ

Traffic Data as Proxy of Business Downtime after Natural Disasters: the Case of Kathmandu

F. De Luca¹, D. Damen², J. Kurton³, M. Wray⁴, R.M. Pokhrel⁵, M.J. Werner⁶

ABSTRACT

Traffic data identified from free, satellite imagery, such as historical imagery available on Google Earth, are collected and employed as possible indicator of business downtime after the 2015 Gorkha Earthquake in Nepal. Business downtime is a crucial factor when assessing losses and it is also of great importance to insurance and reinsurance companies, particularly the downtime of private businesses, for which limited data is available. Currently, indicators of business recovery after natural disaster events either focus on damage or they are directly collected through costly procedures and none of the approaches available quantifies longer term recovery. In many cases, such data, when available, are not easy to access. There is a need for both time- and cost-effective methods to quantify business downtime that are not necessarily derived from physical damage and are able to describe both short-term and, potentially, long-term business recovery. The aim of this quantification refers to the recovery phase rather than the immediate emergency response in the aftermath of a natural disaster. Car and lorry numbers of four areas of Kathmandu were counted from historical images available on Google Earth. These four areas correlated to the four areas in which data related to business closures were obtained through interviews during a field investigation made by the authors in Kathmandu in November 2016 (18 months after the event). Food and health business closure data correlate very satisfactory with the calculated drop in car numbers.

Introduction

Loss estimation is essential to assessing the severity of natural hazards, as well as identifying vulnerability and guiding recovery decisions and processes. The evaluation of economic losses is typically made in terms of monetary losses, casualties and downtime. The definition of downtime in Performance Based Earthquake Engineering (PBEE) is “the time necessary to plan, finance, and complete repairs on facilities damaged in earthquakes or other disasters” [1]. However, this definition relates more to short-term business recovery than the long-term [2]. Business resiliency has been identified as a principal factor for loss estimation and indicators of business interruption that are not related solely to the amount of damage and are indicative of longer-term recovery process are becoming increasingly significant [3].

¹Lecturer, Dept. of Civil Engineering, University of Bristol, Bristol, BS8 1TR (email: flavia.deluca@bristol.ac.uk)

²Senior Lecturer, Dept. of Computer Science, University of Bristol, Bristol, BS8 1UB

³Undergraduate Student Researcher, Dept. of Civil Engineering, , University of Bristol, Bristol, BS8 1TR

⁴PhD Student, Dept. of Computer Science, University of Bristol, Bristol, BS8 1UB

⁵CEO, Earth Investigation and Solutions Nepal Pvt. Ltd, GPO. Box No. 9261, Kathmandu, Nepal

⁶Senior Lecturer, School Earth Sciences, University of Bristol, Bristol, BS8 1TRJ

In the recent past, business recovery has been assessed with one off, large scale surveys and investigations of the disaster affected communities [4]. These procedures are both costly and require substantial amounts of organization and effort. Thus, there is a need for time and cost-effective methods to track business recovery after natural disasters. Statistical data is a useful tool to provide baseline information for comparing “before and after” scenarios, and therefore methods of quantifying recovery are needed [5]. There are two main difficulties surrounding the quantification of business recovery: firstly, not all studies refer to the same definitions of downtime and recovery; and secondly, it is difficult to collect data on the private sector and small businesses. Therefore, most studies in the past focused on public and government businesses for which it is easier to obtain information.

In this study, downtime of private businesses and commercial activities is defined as the time during which the specific activity remained closed after the disaster until returning to normal opening time activity. Noy [6] states that the factors affecting economic recovery from a natural disaster include literacy rate, per capita income, openness to trade, amount of government spending, quality of institutions, foreign exchange reserves, and domestic credit levels. He concludes that developing countries suffer a greater shock to their economies than developed countries and small economies are at much greater risk to indirect consequences than larger economies [6]. For insurance and reinsurance companies, the quantification of business recovery, in particular for the private sector can be of great interest. In developed countries, it can be easier to collect data and build up models for business quantification (e.g., [2]; [3]); while for the case of developing countries the quantification of business recovery in the private sector can be even more challenging. It is therefore assumed that the work shown herein will only be applicable to business recovery in developing countries.

Remote sensing and satellite imagery are very time effective methods used to determine loss estimation, particularly looking at damage. Haghigattalab et al. [7] used high-resolution satellite imaging, such as Quickbird and IKONOS, in order to classify damage and immediate response following the Bam, Iran earthquake in 2003. These images were used to detect damage on roads (such as building debris, presence of cars or collapsed trees), and consequently which roads were blocked. Booth et al. [8] also investigated the use of high resolution remote imagery to accurately demonstrate the damage of buildings after the Haiti 2010 earthquake, by comparing two different sets of imagery with ground observations. These images were obtained from high altitude aircraft with resolutions of 25cm or better and, as a result, are likely to be very costly. Damage detection through satellite information has become very relevant for emergency response [9] and this has determined significant efforts for automatic visual computation on satellite imagery [10].

A focus on road networks as an indicator of economic loss and business downtime has also been noted in current literature, as damage to road networks is responsible for substantial disruption and economic loss. Chang and Nojima [11] developed a method to measure the system performance of road networks after the 1995 Kobe earthquake and used length of network open and distance of accessible travel routes as possible performance indicators. Similarly, Contreras et al. used travel times as a possible indicator of recovery after the 2009 L’Aquila earthquake [12]. Previous investigation into road recovery by calculating the distance of usable roads in an area using free and open telematics data from satellite navigation software was undertaken by Endo and Komori, following the 2011 Tohoku Earthquake [13].

A further study into the use of pedestrian traffic as a suitable proxy for recovery of central building districts was undertaken by Harding and Powell [4], after the Christchurch earthquake in 2010. They conclude, from the initial investigation, that pedestrian footfalls have the potential to be an indicator of business recovery.

There has been a recent increase in investigations into using road networks and remote sensing, including satellite imagery, as ways of assessing business interruption and downtime, as well as damage and recovery levels. Contreras et al., after investigating the use of remote sensing, GIS and ground observations to monitor recovery, recommends the use of Google Earth time series data as an indicator of both change and progress in a post-disaster recovery progress [14].

This study aims to use remote sensing from historical images available in Google Earth to measure long term business recovery by using traffic levels as a proxy. If extensively validated, this methodology would be a cost-effective indicator of business recovery in the short-term and long-term. This approach can then be used to help create loss estimation frameworks. To validate the reliability of the approach, data from interviews made in the city of Kathmandu are collected and compared. The preliminary aspect addressed herein is whether there is a significant correlation between the time different businesses were closed and the “traffic drop” as observed from satellite imagery in Google Earth in the same areas using a very simple regression model for traffic time-series. The traffic drop is intended as an integral quantity of the disruption obtained analyzing the traffic trends after more than one year from the event.

In the following, we firstly provide a general overview of the earthquake event that struck Nepal in April 2015, with focus on the damage observed in the city of Kathmandu (i.e., the main focus of this study). Then, we discuss in detail the methodological approach of this study and how the field data were analyzed and correlated with historical satellite imagery information from Google Earth. Finally, we summarize the general conclusions and further developments of this “proof of concept” study.

The 2015 Gorkha earthquake

The Mw 7.8 Gorkha earthquake occurred on April 25, 2015. Its epicenter was located 77km North West of Kathmandu and the event depth was 15 km. Shaking lasted for two minutes and triggered hundreds of aftershocks, five of which registered Mw above 6. The most significant aftershock occurred on May 12 (approximately two weeks after the mainshock) with the epicenter located in the North East of Kathmandu. The May aftershock was Mw 7.3 and caused significant additional damage. As expected, from the tectonic history of the area, the earthquake’s epicenter was located in the Eastern side of the seismic gap [15]. The Western side of the seismic gap remains unbroken and, therefore, it is highly likely that another major seismic event will occur there in the near future.

Some secondary effects such as landslides and minor liquefaction did take place, however much of these were small scale and very localized, and much of the damage affected buildings. The severity of this damage was related to the topographic and soil conditions of Kathmandu Valley [16]. Fig. 1a shows the map of the average shear-wave velocity in the uppermost 30m (V_{S30}) based on data available from the United States Geological Survey (USGS) and provided in [17]. V_{S30} is used as proxy for site-amplification models in many codes (e.g., [18]), and, in this

framework, it can support damage interpretation given the lack of recorded data. Nepal has a very poor network of strong motion stations in place; only the records from the KATNP station were publicly available after the event. However, the KATNP station is in central Kathmandu, very close to the areas investigated herein, so the intensities discussed will be reasonably accurate (see Fig. 1a). The response spectra recorded at the KATNP station show two main peaks: a short peak in the N-S component at 0.2-0.6s and a larger peak across all components at a period of 4-6s. The shorter peak is due to direct shaking, and the larger peak is mostly due to the basin effects of the Kathmandu Valley [17]. Kathmandu is located within a very deep sedimentary basin, with sediment reaching a maximum thickness of approximately 550m. This basin is made up of thick lacustrine and fluvio-lacustrine deposits (formed in the bottom of ancient lakes) and has a natural dominant period of 1-2s [19]. This is likely to have significantly modified the ground motion of the earthquake and is regarded to be the cause of the amplification at the 4-6s range.

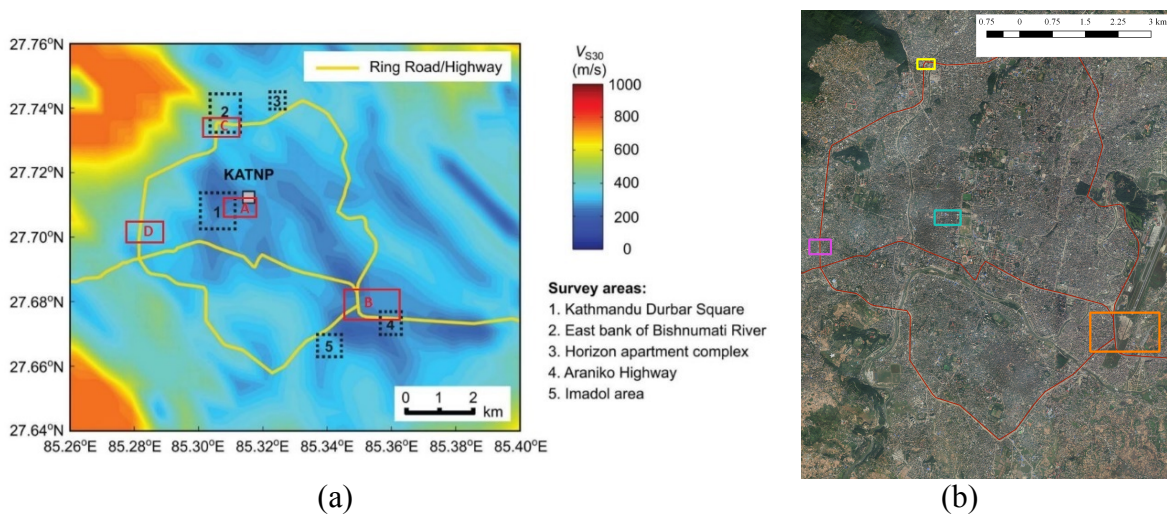


Figure 1. (a) V_{S30} velocity map form USGS, location of KATNP station, survey areas by Goda et al. [17] (indicated as 1-5) and the four zones investigated in this study (indicated as A-D) with regards to the Kathmandu ring road (adapted from [17]); (b) Surveyed areas of this study under satellite imagery map of Kathmandu city cyan (zone A), orange (zone B), yellow (zone C), magenta (zone D).

Damage

The majority of building types in Kathmandu are low to mid-rise buildings which have a natural period of <1 s and so were not affected by the long-period ground motions. It is therefore presumed that the short peak in the North South component at 0.2-0.6s caused the majority of the damage to buildings [17]. Much taller buildings (approximately ten storeys high) have a resonance period of 1-2s and so are much more likely to resonate with the dominant period of the basin and therefore suffer much greater damage. Currently, only historical buildings are likely to fall into this category and a number of high-rise condominium recently built in the urban area.

Unreinforced masonry buildings made up the majority of collapsed buildings in Kathmandu, particularly many historic buildings in Durbar Square. Reinforced Concrete (RC) buildings with masonry infills were more resistant to shaking due to their increased stiffness; these buildings make up approximately 28% of all buildings in urban areas like central Kathmandu [20].

Due to the higher numbers of RC buildings, less buildings were destroyed than in most other areas, but a greater percentage were partially damaged. Very high buildings also suffered significant damage; this can be related to the peculiar peaks in the response spectra of the earthquake.

A damage survey was undertaken by Goda et al. [17] in May 2015 and areas 1, 2 and 4 from Goda et al.'s survey coincide with zones A, C and B investigated in this study, as shown in Fig. 1a and Fig. 1b. Area 1 and zone A are located by Kathmandu Durbar Square, home to the city's historic buildings which suffered severe amounts of damage, some even suffering complete collapse. However, non-historic buildings surrounding Durbar Square were undamaged, some suffered from minor cracking in masonry but remained structurally sound. A large portion of damaged housing in Kathmandu was in zone C, located in the North West of the city. This is likely to be due to the different soil conditions present here. Most of the damage in Kathmandu, in comparison to other districts, was extremely localized. Severe damage likely occurred due to local conditions such as soil type and poor construction practice.

Methodology

Our surveys were undertaken in four parts of central Kathmandu (inside the main ring road, see Fig. 1b) as part of a research field mission to Nepal in November 2016. Once these four areas were defined, the number of cars in these areas over time were counted using historic imagery freely available in Google Earth and provided from third party companies (e.g., DigitalGlobe) as documented from the software. Multiple businesses across certain roads were interviewed and data regarding the length of time they remained closed after the earthquake was obtained. The latitude and longitude of the four corners of areas A-D are shown in Table 1 along with their areas and number of surveyed businesses. Table 1 also provides the length of vehicle accessible roads in each zone, according to two different definitions for normalization of traffic flows. Normalization method 1 treats the main roads and ring road as twice as significant as the local roads and so the lengths of these are doubled. Normalization method 2 only considers the lengths of the major roads within the zones and the local roads are not counted.

Zone A is located next to Kathmandu Durbar Square, near the center of Kathmandu. Only local roads pass through this area and it was expected that low level of traffic is present here. This area experienced some significant damage, mainly to some of the temples in Durbar Square and this damage is likely to be because of both their unreinforced masonry construction and also the height of the buildings suffering from amplification effects [20]. The population density of central Kathmandu is 20,287.3 people/km² according to 2011 census data [21]. Zone B lies to the South of the Tribhuvan International Airport, in an area which had been newly constructed and recorded very little damage. This zone lies at the junction between the ring road and Araniko Highway and it covers the largest area; it is expected to see the highest traffic in this zone. Much of this area falls within the district of Kathmandu, however the Eastern section lies in the municipality of Madhyapur Thimi, which has a much lower population density of 7,572.3 people/km². Zone C is in the Northwest of Kathmandu, with both the Bishnumati River and the ring road running through it. This zone is notably smaller than the others and therefore, despite having a major road running through it, is expected to have the smallest numbers of cars passing through. This area of Kathmandu has alluvial soils and so suffered from more damage than most areas of Kathmandu due to the soil exhibiting amplification effects of the ground motion. This zone also lies in the main district of Kathmandu and therefore has the same population density as zone A. Zone D is in

South West Kathmandu, just South of the Manamati River and also has the ring road running directly through it. This zone lies directly next to the village of Seuchatar which has a very low population density in comparison to Kathmandu, i.e., 4893 people/km².

Table 1. Summary of the location and size of the four zones considered in Kathmandu

| Zone | Coordinate | Latitude (decimal degrees North) | Longitude (decimal degrees East) | Area (km ²) | Road Length (km) | | Number of surveyed businesses |
|-----------|------------|--|--|----------------------------|---------------------|------|-------------------------------------|
| | | | | | A* | B** | |
| Zone A | 1 | 27.705 | 85.308 | 0.19529 | 3.255 | 2.07 | 23 |
| | 2 | 27.705 | 85.314 | | | | |
| | 3 | 27.702 | 85.308 | | | | |
| | 4 | 27.702 | 85.314 | | | | |
| Zone B | 1 | 27.684 | 85.344 | 1.3904 | 11.422 | 2.27 | 29 |
| | 2 | 27.684 | 85.360 | | | | |
| | 3 | 27.676 | 85.344 | | | | |
| | 4 | 27.676 | 85.360 | | | | |
| Zone C | 1 | 27.736 | 85.304 | 0.081576 | 1.781 | 0.48 | 24 |
| | 2 | 27.736 | 85.308 | | | | |
| | 3 | 27.734 | 85.304 | | | | |
| | 4 | 27.734 | 85.308 | | | | |
| Zone D | 1 | 27.699 | 85.279 | 0.163344 | 2.203 | 0.73 | 11 |
| | 2 | 27.699 | 85.284 | | | | |
| | 3 | 27.696 | 85.279 | | | | |
| | 4 | 27.696 | 85.284 | | | | |

*Normalization method 1 **Normalization method 2

Satellite business recovery evidence: “car counting”

In order to investigate a difference in traffic trends before and after the April 25 earthquake, cars were counted from historical imagery between January 2014 and April 2016 (see Fig. 2). Overall, between 2014-2016, 22 historical images were available in Google Earth and of these, two were unusable for all four zones (see the strikethrough dates in Fig. 2). This is due to either being too dark to accurately interpret them or because of cloud cover. In Google Earth, a boundary was drawn between the four coordinates marking the corners of the zone and cars laying within this zone were counted (see Fig. 3). Only cars located completely inside the boundary lines were counted to ensure consistency. Both numbers for parked and moving cars were collected and it was assumed that any car present on a road was moving. Both cars and lorries were present in these images and could be identified by the difference in size and therefore both types of vehicle were counted. There were also many smaller black marks on the roads and it was assumed these were motorbikes or similar, which are very common in Kathmandu. However, because of the difficulty in identifying them accurately, they were omitted.

Fig. 3 shows an example of the vehicles counted for Zone C on two different days. No information was available in relation to the time of day the images were recorded; however, it was assumed that they were all taken at roughly the same time of day. This is because, despite there are differing light levels in the images, the shadows are all facing the same direction in the majority of the images and only vary about 2m in length. It should also be noted that images can only be

taken when the sun is reasonably high in the sky in order to obtain viewable images [22] and so they are likely to be taken roughly at the same time of day, possibly mid-late morning, due to the shadows forming on the west side of the buildings.

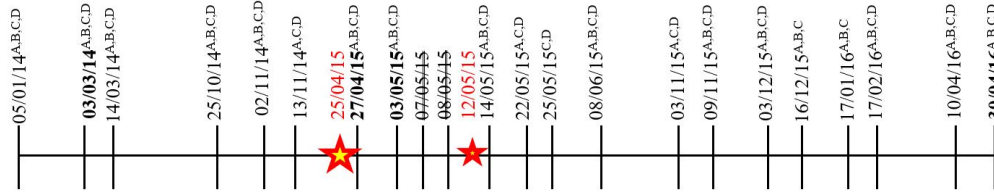


Figure 2. Timeline showing dates of historical images available, including the zones for which they were used, the date of the earthquake and its main aftershock (see the red stars), the unusable images struck through, and in bold the dates used as example in Fig. 3.

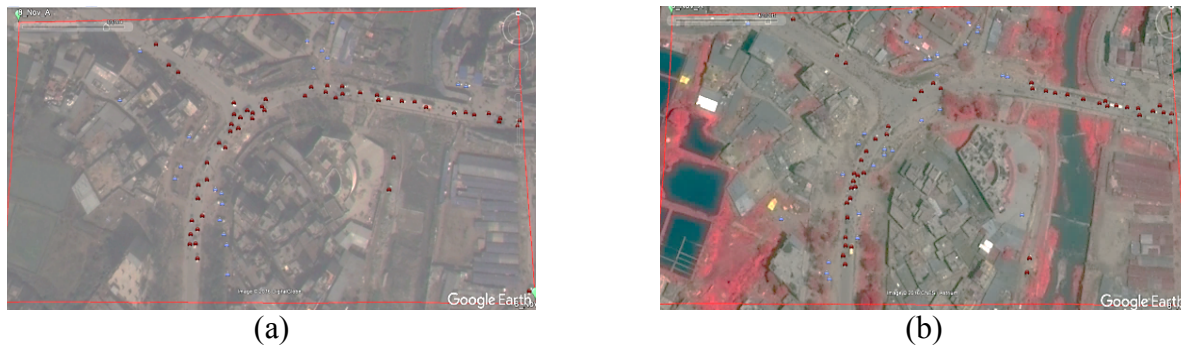


Figure 3. Example of car counting for Zone C for (a) 03/03/14; (b) 27/04/15. Note: pictures have been corrected for improved clarity. (Source Digital Globe through Google Earth).

Field Data

The survey results were compiled into a database to assess the business types, and length and reason of closure in each zone. The trend of most note is the average length of business closure, shown in Fig. 4. The only reason for closure in both zones A and B was due to damage (or an unspecified reason). Damage is the biggest reason for closure in zone D and it was the reason that resulted in the longest closures. A higher percentage of businesses closed due to damage in zones C and D. Damage was responsible for the highest average downtime for zone D. However, a lack of demand was responsible for the longest average business closures in zone C, possibly since it is furthest from the center of Kathmandu. Another important reason for closure is scare; this is only significant in zones C and D. The businesses were split into three different subcategories: “food and health” such as bakeries, groceries or pharmacies; “other commercial businesses” such as manufacturing, clothing and jewelry shops; and “services”, such as banks or travel agencies. Fig. 4 shows the distribution of downtime within these subcategories. Only zones B and D had services and this business type seemed to be the most significant contribution to business closure for zone D. On the other hand, due to the lack of data for these categories in zones A and C they cannot be used in relation to the traffic flow estimated in the four zones.

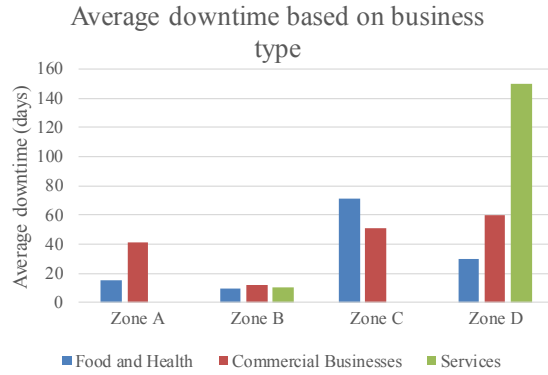


Figure 4. Average downtime for each zone and split according to the three business categories considered as per data collected by the authors in November 2016.

Preliminary Data Analysis

Moving and parked car numbers are collected; however, analysis was only made on the total number of cars. This distinction has been made for potential further automatization of the traffic flow counting and to have the possibility, in future studies, to double check if moving cars are enough as proxy for business recovery time. An idealized version of these trends was then created (see Fig. 5a). There appeared to be two different trends within each zone: a fluctuation around an average value before the earthquake, then an increasing linear trend after the earthquake. Treating the car numbers before and after the earthquake as two different data sets resulted in a straight-line average up to the earthquake and an increasing linear trend after it, resulting in the computation of a drop (i.e., the step in Fig 5a). The drops for each zone were then normalized by dividing them by the length of the roads present in each zone. Two different definitions of road length are used in order to obtain two different normalization methods. Normalization 2 is the most suitable method. In this method, zone B has the most cars per km out of all the zones and this reflects the fact that the extremely busy ring road makes up most of the road lengths in zone B. Similarly, zone A is the only area without the ring road running through it and it is expected to have much less dense traffic, which is reflected in this normalization by having the lowest car/km by a significant amount.

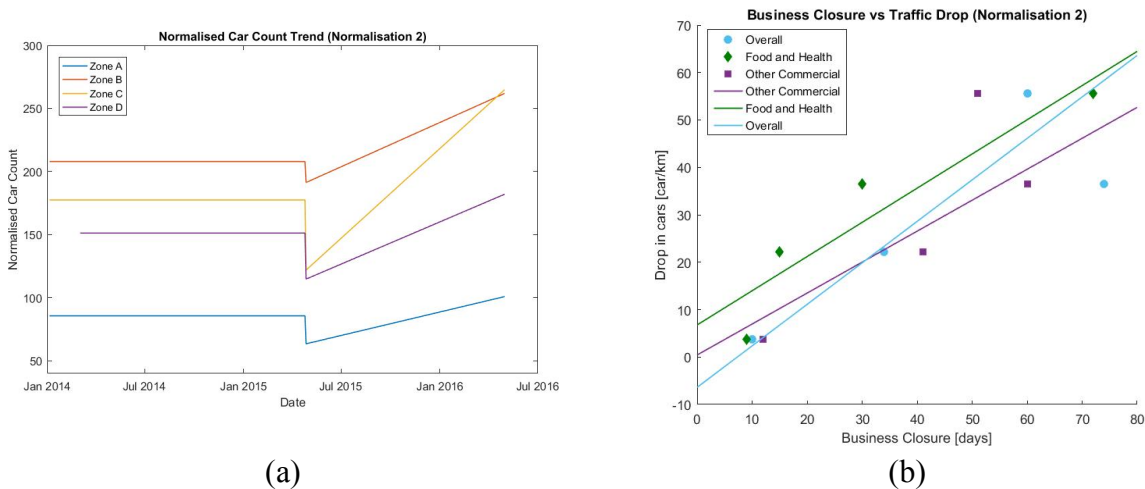


Figure 5. (a) Idealized trend for normalization 2 and (b) correlation plot of businesses closure and drop in car numbers.

The drop in car number is then used as a proxy for downtime and compared to the average downtime per area. This drop does not represent necessarily a reduction of traffic right after the event (e.g., hours or days) but an integral measure of the traffic disruption over a longer period after the event (e.g., one year) resulting from the modelling of the trend before (constant) and after (linear) making it suitable to be correlated with the business downtime. It is worth noting that traffic flows in the hours or the first days after a strong earthquake do not necessarily go suddenly down and the drop trend can appear after weeks. To gain an accurate representation of business recovery, a comparison was drawn between overall average downtime and the subcategories of Food and Health and Commercial businesses (see Fig. 5b). To investigate the strength of correlation, Pearson's correlation coefficient for each normalization method was calculated. The coefficients obtained for both normalization methods were positives, as shown in Table 2.

Table 2. Correlation coefficients for the two normalization methods.

| | Overall | Food and Health | Commercial |
|---------------------------|----------------|------------------------|-------------------|
| Normalisation 1 | 0.7570 | 0.9032 | 0.6210 |
| Normalisation 2 | 0.8434 | 0.9336 | 0.8306 |
| Normalisation Area | 0.6012 | 0.7891 | 0.7054 |

Conclusions and Developments

The initial results of this study suggest a very strong positive correlation between the drop in traffic after the earthquake and the average downtime experienced in an area by small private businesses. Although very limited amount of data could be obtained to make this correlation, the strength of it suggests that it can be valid, even if further analyses are necessary on the variability of the traffic data to assess the significance of the regression on these trends. Highest correlation was found between the drop in traffic and the downtime of businesses in the food and health category, (having a correlation coefficient of 0.9336). Food and health businesses are those fundamental for any real recovery of business activity in an area and this strong correlation confirms an intuitive observation. To test whether this result is a fluke, it is suggested that the same normalization methods are applied to an area with similar traffic levels and level of development, with a random date of a supposed event. This approach can be employed in urban areas where the traffic levels are significant, so that any decrease in numbers is clear, and it is best applicable to developing countries where car numbers are more likely to represent the activity of local businesses. In fact, in developed countries, the absence of cars does not necessarily represent a lack of business activity given the presence of alternative means of transport such as undergrounds or similar. Moreover, a sufficient number of Google Earth historical images is only available for developing countries, so any further application and validation, at this stage, can be done only in developing countries.

Acknowledgments

This work was funded by EPSRC under the University of Bristol Global Challenge Institutional Sponsorship project "Post-Natural Disaster downtime quantification after earthquakes through remote sensing: the case of the M_w 7.8 Gorkha 2015 (Nepal)" (EP/P510920/1).

References

1. Comerio, M.C. Estimating downtime in loss modelling. *Earthquake Spectra* 2006; **22**(2): 349-365.

2. Webb, G.R., Tierney, K.J. and Dahlhamer, J.M. Predicting long-term business recovery from disaster: a comparison of the Loma Prieta earthquake and Hurricane Andrew. *Global Environmental Change Part B: Environmental Hazards* 2002; **4**(2): 45-58.
3. Rose, A. and Lim, D. Business interruption losses from natural hazards: conceptual and methodological issues in the case of the Northridge earthquake. *Global Environmental Change Part B: Environmental Hazards* 2002; **4**(1): 1-14.
4. Harding, A.J.M. and Powell, F.I. Variations in Pedestrian Traffic Count in Christchurch due to the September 2010 Darfield (Canterbury) Earthquake. *Proceedings of the Ninth Pacific Conference on Earthquake Engineering: Building an Earthquake-Resilient Society* April 2011; 14-16.
5. Chang, S.E. Urban disaster recovery: a measurement framework and its application to the 1995 Kobe earthquake. *Disasters* 2010; **34**(2): 303-327.
6. Noy, I. The macroeconomic consequences of disasters. *Journal of Development economics*, 2009; **88**(2): 221-231.
7. Haghhighattalab, A., Mohammadzadeh, A., Valadan Zoej, M. J., & Taleai, M. Post-earthquake road damage assessment using region-based algorithms from high-resolution satellite images. In *Image and Signal Processing for Remote Sensing XVI (Vol. 7830)*, October 2010.
8. Booth, E., Saito, K., Spence, R., Madabhushi, G. and Eguchi, R.T. Validating assessments of seismic damage made from remote sensing. *Earthquake Spectra* 2011; **27**(S1): S157-S177.
9. Ghosh, S., Huyck, C. K., Greene, M., Gill, S. P., Bevington, J., Svekla, W., ... & Eguchi, R. T. (2011). Crowdsourcing for rapid damage assessment: The global earth observation catastrophe assessment network (GEO-CAN). *Earthquake Spectra*, 27(S1), S179-S198.
10. Trekin, A., Novikov, G., Potapov, G., Ignatiev, V., & Burnaev, E. (2018). Satellite imagery analysis for operational damage assessment in Emergency situations. arXiv preprint arXiv:1803.00397.
11. Chang, S.E. and Nojima, N. Measuring post-disaster transportation system performance: the 1995 Kobe earthquake in comparative perspective. *Transportation Research Part A: Policy and Practice* 2001; **35**(6): 475-494.
12. Contreras, D., Blaschke, T., Kienberger, S. and Zeil, P. Spatial connectivity as a recovery process indicator: The L'Aquila earthquake. *Technological Forecasting and Social Change* 2013; **80**(9): 1782-1803.
13. Endo, N., & Komori, H. Regional difference on road recovery in Iwate prefecture following the 2011 Tohoku earthquake. In *Proceedings of The World Congress on Engineering and Computer Science* 2015; 162-167.
14. Contreras, D., Blaschke, T., Tiede, D. and Jilge, M. Monitoring recovery after earthquakes through the integration of remote sensing, GIS, and ground observations: the case of L'Aquila (Italy). *Cartography and Geographic Information Science* 2016; **43**(2): 115-133.
15. Lizundia, B., Shrestha, S.N., Bevington, J., Davidson, R., Jaiswal, K., Jimée, G.K. and Ortiz, M. EERI earthquake reconnaissance team report: M7. 8 Gorkha, Nepal earthquake on April 25, 2015 and its aftershocks. *Earthquake Engineering Research Institute* 2016 Available at: <http://www.eqclearinghouse.org/>
16. Gautam, D. and Chaulagain, H. Structural performance and associated lessons to be learned from world earthquakes in Nepal after 25 April 2015 (Mw 7.8) Gorkha earthquake. *Engineering Failure Analysis* 2016; **68**: 222-243.
17. Goda, K., Kiyota, T., Pokhrel, R., Chiaro, G., Katagiri, T., Sharma, K. and Wilkinson, S. The 2015 Gorkha Nepal Earthquake: Insights from Earthquake Damage Survey. *Frontiers in Built Environment* 2015; **1**:8.
18. CEN. European standard EN1998-1:2004. Eurocode 8: design of structures for earthquake resistance. Part 1: general rules, seismic actions and rules for buildings. *Comité Européen de Normalisation* 2004; Brussels.
19. Sakai, T., Gajurel, A. P., Tabata, H., & Upreti, B. N. Small-amplitude lake-level fluctuations recorded in aggrading deltaic deposits of the Upper Pleistocene Thimi and Gokarna formations, Kathmandu Valley, Nepal. *J Nepal Geol Soc* 2001; 25(special issue): 43-52.
20. Aon Benfield. 2015 Nepal Earthquake Event Recap Report. September 2015.
21. National Bureau of Statistics. Kathmandu Valley (Nepal): Cities, Municipalities and Villages - Population Statistics in Maps and Charts. 2011
22. Taylor, F. About Google Earth Imagery. *Google Earth Blog* 2008. Available at: https://www.gearthblog.com/blog/archives/2009/03/about_google_earth_imagery_1.html.